

Alpha hit frequency due to radon decay products in human lung cells

D. NIKEZIC^{†‡} and K. N. YU^{†*}

(Received 8 September 2000; accepted 15 December 2000)

Abstract.

Purpose: To calculate the hit probabilities by α -particles emitted by radon progeny for basal and secretory cell nuclei in the epithelium of the human tracheobronchial tree.

Materials and methods: The equilibrium activities on the surface of airway tubes were calculated using the ICRP66 model. The stopping-power and ranges of α -particles in tissue were adopted from ICRU49. A semi-analytical method for determining the α -particle fluence rate in tissue was applied. The distributions of secretory and basal cells throughout the tracheobronchial tree were as given by Mercer *et al.* (1991).

Results: The probability to hit basal cell nuclei is three-to-four times smaller than for secretory cell nuclei in the bronchial region (BB). However, the total number of traversed basal cell nuclei is greater because of the larger volume abundance of basal cells in BB. The total number of secretory cell nuclei hit in the bronchiolar region (bb) is larger than that in BB because the volume abundance of secretory cells in bb is larger than that in BB.

Conclusions: Basal cells are more sensitive to α -radiation than secretory cells. This finding is based on the analysis of the relative number of cell hits and the relative frequencies of lung cancer induction in BB and bb.

1. Introduction

The probability that α -particles emitted by radon progeny in the mucous layer of the human lung can hit epithelial cells has been estimated by Harley (1988) and Hui *et al.* (1990). Since then new information has emerged on radon dosimetry (ICRP 1994, Reineking *et al.* 1994, Marsh and Birchall 2000). The hit probabilities have been recalculated here using the new information. The Human Respiratory Track Model ICRP66 (ICRP 1994) is used as the starting point. In addition, the information on the distribution of sensitive cells was employed with the depth of epithelial tissue given by Mercer *et al.* (1991).

2. Method of calculation

Since the program used in ICRP66 is not commercially available, the present authors have developed

their own program in FORTRAN90. This was validated against that of Marsh and Birchall (2000) by comparing the sensitivity analysis results of different parameters using the same data.

2.1. Deposition model

The ICRP66 model calculated deposition of radon progeny in the respiratory tract. The human respiratory tract is treated as a series of five filters (or regions), each lowering the concentration of aerosols (and thus radon progeny) in the air passing throughout the lung: the extrathoracic (ET), bronchial (BB), bronchiolar (bb), alveolar–interstitial (AI) and lymphatic (L) regions. These regions have their own characteristics regarding deposition, clearance, as well as some other important features. Here, the deposition regions are denoted by $ET1_{insp}$, $ET2_{insp}$, BB_{insp} , bb_{insp} , AI , bb_{exp} , BB_{exp} , $ET2_{exp}$ and $ET1_{exp}$, where the subscripts ‘insp’ and ‘exp’ refer to inspiration and expiration, respectively. There are nine regions for nasal breathing but only seven for mouth breathing ($ET1_{insp,exp}$ excluded). Regional deposition efficiencies are given in the form of algebraic expressions in ICRP66. These expressions have been used here for the calculation of deposition efficiencies and activities deposited in different regions of the respiratory tract for monodispersed particles. However, atmospheric aerosols have multimodal log–normal distributions. Radon progeny principally exist as unattached atoms in the form of fine clusters and atoms attached to natural aerosols. Summation of data for monodispersed particles is required to compute the amount of deposited radon progeny in different regions of the tracheobronchial (TB) tract. The deposition thus obtained was in good agreement with ICRP66.

Reineking *et al.* (1994) described the attached mode as the sum of three activity size distributions: (1) nucleation mode, (2) accumulation mode and (3) coarse mode. According to Marsh and Birchall (2000) the fractions of total potential α energy concentration (PAEC) in different modes are: 8% in unattached mode (u), 25.8% in nucleation mode (N), 64.4% in accumulation mode (A) and 1.8% in coarse mode

*Author for correspondence; e-mail: peter.yu@cityu.edu.hk

[†]Department of Physics and Materials Science, City University of Hong Kong, Tat Chee Avenue, Kowloon Tong, Kowloon, Hong Kong.

[‡]On leave from University of Kragujevac, Faculty of Science, 34000 Kragujevac, Yugoslavia.

(C). The median and geometric standard deviation (GSD) of the distributions used in calculations are: $AMTD_u = 0.9$ nm, $GSD_u = 1.3$; $AMAD_N = 50$ nm, $GSD_N = 2$; $AMAD_A = 250$ nm, $GSD_A = 2$; $AMAD_C = 1500$ nm, $GSD_C = 1.5$. (AMTD and AMAD stand for activity median thermodynamic diameter and activity median aerodynamic diameter, respectively.)

2.2. Clearance model and calculation of the equilibrium activity

ICRP66 divided the respiratory tract into 16 clearance compartments. Marsh and Birchall (2000) simplified this model to ten clearance compartments to reduce computational time. Here the original 16-compartment model was used to compute equilibrium activities of radon progeny in all compartments. A set of differential equations shown in equation (1) has been developed for the three relevant radon progeny and for all compartments

$$\begin{aligned} \frac{dN_{ij}}{dt} = & \frac{B_{ij}}{\lambda_i} + A_{i-1j} + \sum_k m_{k \rightarrow j} N_{i,k} \\ & - \sum_n m_{j \rightarrow n} N_{ij} - (\lambda_i + \lambda_b) N_{ij} \\ & i = 1, 2, 3 \text{ and } j = 1, \dots, 16, \end{aligned} \quad (1)$$

where N_{ij} is number of atoms of the i th progeny in the j th compartment, B_{ij} is the deposited activity per unit time of the i th radon progeny in the j th compartment, A_{i-1j} is the activity of $(i-1)$ th radon progeny in the j th compartment, λ_i is decay constant of i th progeny and λ_b the blood transfer constant. The first summation in equation (1) represents the clearance of the i th progeny from all other regions k to region j , while the second sum (preceded with a negative sign) represents the clearance of the i th progeny from the j th compartment to all other compartments n .

Equilibrium corresponds to $dN_{ij}/dt=0$, where equation (1) becomes a system of linear equations which can be solved by computer. The solutions give the number of radon progeny atoms and thus the activities of radon progeny in the clearance compartments.

The BB and bb compartments (in ICRP66 terminology) are of the greatest concern. BB denotes the bronchial region, i.e. generations one to eight (trachea is denoted as the zeroth generation), and bb denotes the bronchiolar region, i.e. generations nine to 16. The BB and bb compartments are further divided into BB_1 , BB_2 , bb_1 and bb_2 , where the subscripts '1' and '2' denote fast and slow clearance, respectively.

2.3. Calculation of the effective dose

Equilibrium activities of radon progeny in different compartments are multiplied by the absorbed dose per unit activity (or absorbed fraction of α -particle energy) to give the absorbed dose in the sensitive cells.

Basal cells and secretory cells are the two types of sensitive cells considered here. According to ICRP66, basal cells are present in BB only while secretory cells exist in all 16 generations of the TB tree. The dose D_{BB} in BB is obtained by summing the dose for basal cells $D_{BB,basal}$ and that for secretory cells $D_{BB,sec}$, with the weighting factor 0.5 assigned to both types of cells (i.e. assuming equal sensitivities for basal and secretory cells), so

$$D_{BB} = 0.5 D_{BB,basal} + 0.5 D_{BB,sec} \quad (2)$$

The dose in bb is equal to the dose $D_{bb,sec}$ in secretory cells of this region. The total dose D_{TB} in the TB tree is then obtained as the weighted sum of the doses in BB and bb, with the weighting factors 0.333

$$D_{T-B} = 0.333 D_{BB} + 0.333 D_{bb} \quad (3)$$

D_{TB} is then multiplied by the quality factor 20 for α -particles and the weighting factor 0.12 for the lung to give the effective dose. The dose conversion factor (DCF, effective dose per unit exposure in the unit mSv/WLM) is obtained on dividing D_{TB} by the exposure to radon progeny.

2.4. Validation of the program LUNGDOSE

The results generated from the present program, called LUNGDOSE, were compared with those of Marsh and Birchall (2000) who performed sensitivity analyses of DCF on different parameters by varying each parameter in turn around its 'best estimate' while keeping all other parameters at their best estimates for a home environment. Doses in BB and bb were calculated using LUNGDOSE with the best-estimate parameters given by Marsh and Birchall (2000). The results are given in table 1, which shows the comparison for $D_{BB,basal}$, $D_{BB,sec}$ and D_{bb} . The values for BB agree very well, while that for bb obtained by LUNGDOSE is $\sim 14\%$ larger (the origin of the difference is not clear). LUNGDOSE gives a somewhat larger thoracic dose (129 compared with 123 mSv/WLM) and a few percent larger DCF (15.58 compared with 15 mSv/WLM). Considering the complexity of the calculations involved, there is good agreement between the results of LUNGDOSE and those of Marsh and Birchall (2000).

Table 1. Absorbed doses in different lung regions calculated using best estimates of parameters for a home environment.

Target issue	Marsh and Birchall (2000) (mGy/WLM)	Present work (mGy/WLM)
Bronchial basal cells, $D_{BB,bas}$	5.4	5.44
Bronchial secretory cells, $D_{BB,sec}$	12.4	12.47
Bronchial dose ($0.5 D_{BB,bas} + 0.5 D_{BB,sec}$)	8.9	8.95
Bronchiolar D_{bb}	9.2	10.54
Thoracic (mSv/WLM)	123	129.8
Total DCF (mSv/WLM)	15	15.58

2.5. Determination of α -particle fluence rate in the tissue

The following model was developed to determine the α -particle fluence rate in the wall of an airway tube.

2.5.1. Geometry: The geometry model used is shown in figure 1. The airway tube is represented by a cylindrical tube with an inner radius r . The fluence rate is calculated at point A at depth a in the tissue (the distance is measured from the inner surface of the tube, i.e. from the top of the mucous layer). ICRP (1994) recommended five distinct volumetric sources in BB and bb. Only two are considered here, namely the mucous gel and sol layer. The activities in other sequestered and chemically bound sources

are much smaller. Since these sources are volumetric, a three-dimensional model has been developed to calculate the particle fluence rates. Alpha-emitters are distributed between the two cylinders with radii R_1 and R_2 . A tangent t is drawn from the point A on the circle with radius r , and the intersections between the tangent t and circles with radii R_1 and R_2 determine the angles ϕ_1 and ϕ_2 . The tangent t (and angles ϕ_1 and ϕ_2) determines the far wall and the near wall. The fluence rate in the small sphere with diameter d_{sp} around A (indicated as the black circle around A) is calculated. This is first calculated from an infinitesimally small volume around point C in the cylindrical coordinate system with coordinates ρ , ϕ and z . Point B is the projection of point C onto the x - y plane. R is the α -particle range in tissue. The line L is the intersection between the sphere with A as centre and R as radius, and the cylinder with radius R_2 . The activity dA in a small volume element around C is given by

$$dA = A_V \rho \, d\rho \, d\phi \, dz \tag{4}$$

where A_V is the volume-specific activity (assumed to be 1 disintegration μm^{-3}). The near- and far-wall cases are considered. The tangent t defines near-wall cases as those with the emitted α -particles not passing through the air cavity so their ranges are completely in the tissue. Particles emitted from the far wall traverse the air cavity and their paths are partially in air and partially in tissue.

The α -particle fluence rate $d\Phi$ at point A, from the source in an elementary volume C at the distance l , is given as

$$d^3\Phi = \frac{dA}{4\pi l^2} = \frac{A_V \rho \, d\rho \, d\phi \, dz}{4\pi AC^2} \tag{5}$$

where the distance $l = AC$ is calculated by

$$AC^2 = z^2 + (a+r)^2 + \rho^2 - 2(a+r)\rho \cos\phi \tag{6}$$

The condition $AC < R$ is observed in the calculations (R is the α -particle range). The total fluence rate Φ_u per unit volume activity, at point A can be found as a triple integral

$$\Phi_u = \frac{\Phi}{A_V} = \int_{-L}^L \int_{R_1}^{R_2} \int_0^{2\pi} \frac{\rho \, d\rho \, d\phi \, dz}{4\pi \cdot AC^2} \tag{7}$$

and is expressed as particles $\mu\text{m}^{-2} \text{s}^{-1}$ per Bq μm^{-3} . A computer program ALPHA_FLUX was developed to solve the integrals numerically. The variables ρ , ϕ and z were varied between the limits shown in equation (7) with the steps: $\Delta\phi = 0.001^\circ$ for near-wall cases and $\Delta\phi = 1^\circ$ for far-wall cases; $\Delta z = 1 \mu\text{m}$ and $\Delta\rho = 1 \mu\text{m}$.

ALPHA_FLUX can also be used to calculate the

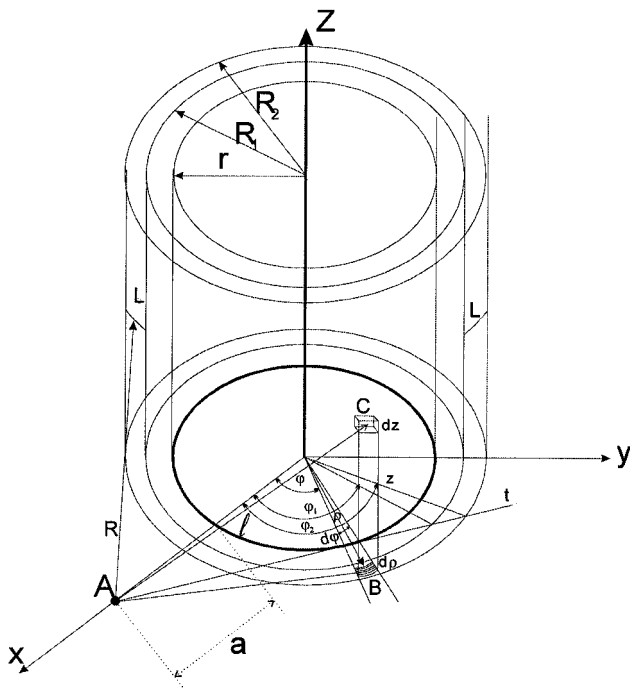


Figure 1. Geometry used for the calculation of α -particle fluence rate.

energy imparted to the sphere around point A and to determine the absorbed fraction (AF) of α -particles in tissue. However, for such calculations the integrand in equation (7) should be multiplied by the stopping power of α -particles after traversing the tissue equivalent distance between A and C, and with the average random chord length through the spherical volume of interest. $2d/3$ has been used as the average random chord length where d is the cell nucleus diameter. Comparing the resulting AF with those of the ICRP validated ALPHA_FLUX. The stopping powers and ranges of α -particles in tissue given in ICRU49 (1993) were used in these calculations. The results obtained by the ALPHA_FLUX were also compared with the results given by NRC (1991). Instead of the absorbed fraction, however, NRC used the dose coefficient given by the absorbed dose (nGy) per 1 disintegration cm^{-2} . Recalculation of AF in terms of the dose coefficient is possible and the results of the present program are in good agreement with the results given by NRC (1991).

As an illustration, the decrease in the α -particle fluence rate in BB with the depth in the tissue is shown in figure 2. There are four curves here, one pair for 6 MeV α -particles and the other pair for 7.69 MeV α -particles.

2.6. Calculation of hit frequencies

Calculations have been performed for the following α -particle sources:

- In BB: BB₁ and BB₂ for 6 MeV and 7.69 MeV α -particles.

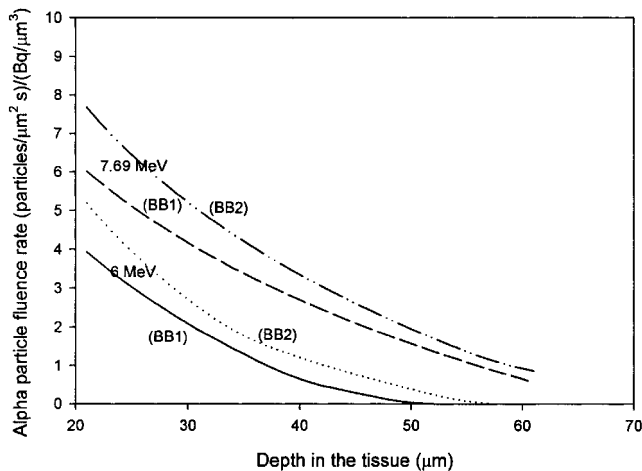


Figure 2. Variation of α -particle fluence rate with the depth of the tissue. Alpha sources are in BB₁ (fast-clearance mucus) or BB₂ (slow-clearance mucus). The fluence rate is given in particles/ $(\mu\text{m}^2 \text{ s})$ per Bq μm^{-3} .

- In bb: bb₁ and bb₂ for 6 MeV and 7.69 MeV α -particles.

The α -particle fluence rate at a depth in the tissue was multiplied by the cross-sectional area of cell nuclei to give the normalized hit frequency (number of hits/cell nucleus per emitted particle in μm^3). Subsequent tasks include determination of equilibrium activities of radon progeny in different clearance compartments (BB₁, BB₂, bb₁ and bb₂) and the number of α -particles N_α ($=A_v \times t$, where A_v is the equilibrium volumetric activity and t is the time of exposure) emitted for the exposure of 1 WLM. Equilibrium activities of radon progeny were determined by LUNGDOSE. The product of the normalized hit frequencies and N_α gave the number of hits of cell nuclei for an exposure of 1 WLM.

3. Results

3.1. Basal cells

The diameter of the basal cell nucleus was taken as $9 \mu\text{m}$. According to ICRP66, basal cells are situated between 46 and $61 \mu\text{m}$ from the top of the mucus. However, the distribution of basal cell nuclei was not given in ICRP66. Mercer *et al.* (1991) gave the volumetric distributions of the cells and cell nuclei, and their distributions of basal and secretory cell nuclei is shown in figure 3. The basal cell nuclei largely follow a triangular distribution. In the present work, the triangular distribution of Mercer *et al.* (1991) was adopted for the basal cell nuclei. The distribution started at $46 \mu\text{m}$ and ended at $61 \mu\text{m}$, with the peak value at $59 \mu\text{m}$ (accounting for 21%; also given by Mercer *et al.* 1991). The number of α -particle hits of basal cell nuclei at a particular depth is thus weighted according to this triangular

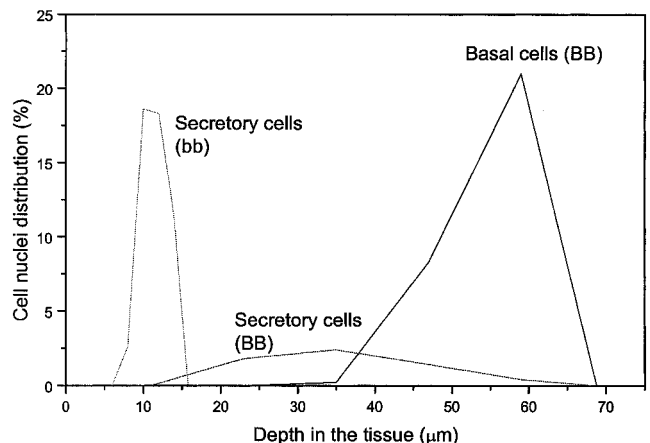


Figure 3. Volumetric distribution of nuclei of basal and secretory cells in BB and bb derived from Mercer *et al.* (1991).

distribution. We obtained 1.084×10^{-2} α -particle hits per cell nucleus for an exposure of 1 WLM. This is sensitive to the starting point of the triangular distribution. For comparison, if the original distribution given by Mercer *et al.* (1991) is applied, it becomes 1.2×10^{-2} .

3.2. Secretory cells

Secretory cells are present in both BB and bb. The depth distributions of secretory cells are different in these two regions.

3.2.1. *BB*: The diameter of secretory cell nuclei is $9 \mu\text{m}$ in this region. According to Mercer *et al.* (1991) the secretory cell nuclei exist between 11 and $65 \mu\text{m}$ below the top of the mucus. In ICRP66, the secretory cell layer started at $21 \mu\text{m}$ and ended at $51 \mu\text{m}$, with no cell distribution or abundance given. The distribution of secretory cell nuclei is flatter than that for basal cells. The secretory cells were taken to be homogeneously distributed from 21 to $51 \mu\text{m}$, and obtained 3.88×10^{-2} α -particle hit per secretory cell nucleus/WLM.

The hit probability is thus three to four times larger for secretory cells than for basal cells. This is expected because secretory cells are closer to α -particle sources and they are present in the region where the α -particle fluence rate is larger. However, *the total number of hits* of secretory cell nuclei by α -particles might not be larger than for basal cell nuclei due to the significantly larger volume abundance of basal cells in BB.

3.2.2. *bb*: The diameter of secretory cell nuclei is $8 \mu\text{m}$ in this region. Secretory cells are situated in bb from 10 to $18 \mu\text{m}$ below the top of the mucus (ICRP66). Mercer *et al.* (1991) gave results for terminal bronchioles (the diameter of bronchiolar tubes is $9.8 \mu\text{m}$), which are also shown in figure 3. The average abundance in these smallest bronchioles is $\sim 10.3\%$. However, the abundance of secretory cells in small bronchi is only 0.8% . It was assumed that the abundance of secretory cell nuclei increased linearly with the number of generations in bb, and 5% was accepted. The volume abundance of secretory cells in bronchioles is significantly larger than that in BB. A rectangular distribution of secretory cells in bb was adopted, which started from $10 \mu\text{m}$ and ended at $18 \mu\text{m}$. Such assumptions gave a hit probability of 3.29×10^{-2} (hits/secretory cell nucleus)/WLM in this region, which is slightly smaller than the value in BB.

3.3. Estimation of the relative number of hit cell nuclei

The actual number of hit nuclei depends on the number of nuclei. The number of basal and secretory cells per cm^2 is unknown. According to Mercer *et al.* (1991), secretory cell nuclei occupy $\sim 2\%$ of the volume in larger bronchi, while in smaller airway tubes it becomes $\sim 1\%$. The volume abundance of basal cells is much larger ($\sim 20\%$) in BB while they are absent in bb. Estimation of the ratio between the numbers of secretory and basal cells can be found by comparing the areas under the curves for basal and secretory cells in figure 3. The area for basal cells is about five times larger than that for secretory cells, so there are about five times more basal cells than secretory cells in BB.

The hit probability for secretory cell nuclei is 3.58 times larger than that for basal cell nuclei. Therefore the total number of hit nuclei of secretory cells and basal cells should be in the ratio $3.58/5 = 0.71$. Since the abundance of both basal and secretory cells decreases through BB, it can be assumed that the number of hit basal cell nuclei N_{bas} is larger than the number, $N_{\text{BB,sec}}$, of hit secretory cell nuclei through BB by the same proportion, giving $N_{\text{bas}}/N_{\text{BB,sec}} \cong 1.41$.

In smaller-airway paths (considered as bb) the hit probability is 3.29×10^{-2} . The abundance of secretory cell nuclei is larger in this region than in BB. The average abundance in larger bronchi is 1.2% , in smaller bronchi 0.8% and terminal bronchioles is 10% . Thus, there are five times more secretory cells in bb (per unit surface) than in BB. The relative number of hit secretory cell nuclei in bb to BB per unit surface is $5 \times 3.29/3.88 \approx 4.23$. According to ICRP66, the surface areas are $S_{\text{BB}} = 290 \text{ cm}^2$ and $S_{\text{bb}} = 2400 \text{ cm}^2$, so the volumes of the secretory layers are $290 \times 30 \times 10^{-4} \text{ cm}^3$ in BB and $2400 \times 8 \times 10^{-4} \text{ cm}^3$ in bb (30 and $8 \mu\text{m}$ are the thickness of secretory layers in BB and bb, respectively). The ratio of the numbers of secretory cell nuclei hit by α -particles in bb and BB is then $4.23 \times 2400 \times 8/290 \times 30 \cong 9.34$. In other words, for each secretory cell nucleus hit by α -particle in BB, there will be on average nine to ten nuclei hits in bb. The result is expected since there are far more secretory cells in bb than in BB (the surface area is eight times larger and the abundance is also larger than those in BB) and the secretory cells in bb are closer to the α -particle sources.

4. Discussion and conclusion

Harley (1988) found that one of 100 sensitive *cells* (but not their nuclei) would be hit by an α -particle

for an exposure of 1 WLM. The present calculations show the average number of traversals of *nuclei* of sensitive cells (nuclei of basal and secretory cells in BB+ nuclei of secretory cells in bb) is $(1.084 + 3.88 + 3.29)/3 \times 10^{-2} \cong 2.75 \times 10^{-2}$ for an exposure of 1 WLM. In other words, 2.75% of the cell nuclei on average will be hit for an exposure of 1 WLM, which is significantly larger than Harley's value.

To compare the present results with those of Hui *et al.* (1990), an exposure of 8.45 WLM was employed, as it was used by Hui *et al.* Our number of hit basal cell nuclei is $1.084 \times 10^{-2} \times 8.45 = 0.099$, whereas Hui *et al.* gave 0.1–0.15 for basal cell nuclei, so the present result is at the lower end of their range. On the other hand, the average number of α -particle hits per secretory cell nuclei/WLM in BB and bb is $(3.88 + 3.29)/2 \times 10^{-2} = 3.58 \times 10^{-2}$, so the number of hit secretory cell nuclei is 0.3 for an exposure of 8.45 WLM. Hui *et al.* (1990) gave the range 0.1–0.25, so the present value is higher than their upper limit. Nevertheless, the methodology employed by Hui *et al.* was completely different from the present one. They used a 'tube' geometry model, and the deposition and clearance models as well as the reference atmosphere were also different. In their work, the depths of basal cells were determined according to the airway diameter.

According to ICRP66 there are four main cancer types in the TB tree: squamous cell carcinoma, small cell carcinoma, adenocarcinoma and large cell carcinoma (table 2). The first column gives the cancer type while the second gives the relative frequency of the respective cancer type to the total number of cancer in the TB tree. The third–fifth columns give the portion of a specific cancer type originating from a particular region in the TB tree. Therefore $\sim 60\%$ of lung cancers originate in BB and 40% in bb. Here, the small contribution of 1.25% from AI is neglected. p_{bas} and p_{sec} denote the induction probabilities of any type of cancer per one traversal of basal cell nucleus

or secretory cell nucleus, respectively. Thus the number P_{BB} of cancers in BB is given as

$$P_{\text{BB}} = p_{\text{bas}}\mathcal{N}_{\text{bas}} + p_{\text{sec}}\mathcal{N}_{\text{BB,sec}} \quad (8)$$

The total number P_{Total} of cancer incidences in BB+ bb (assuming equal sensitivities of secretory cells in bb and BB to α radiation) is

$$P_{\text{TOTAL}} = p_{\text{bas}}\mathcal{N}_{\text{bas}} + p_{\text{sec}}\mathcal{N}_{\text{BB,sec}} + p_{\text{sec}}\mathcal{N}_{\text{bb,sec}} \quad (9)$$

where \mathcal{N} is the number of nuclei traversed. Based on information in table 2, the ratio $P_{\text{BB}}/P_{\text{Total}} = 0.6$, and by combining equations (8) and (9), the relative sensitivity of basal cells to secretory cells is

$$\frac{p_{\text{bas}}}{p_{\text{sec}}} \approx 10 \quad (10)$$

This result shows that basal cells are much more sensitive to α radiation than secretory cells.

If the above estimation is correct (even roughly) some more questions deserve further attention:

- Is the number of nuclei hit by α -particles relevant for the estimation of cancer incidence?
- Is it possible that the sensitivity of secretory cells in BB is different from that of secretory cells in bb? The dimensions of secretory cell nuclei are different in BB and bb.
- If basal and secretory cells are not equally sensitive to α -particles, should we adopt different weighting factors for basal and secretory cells rather than assuming them to be the same as in equation (2)?

Acknowledgements

The present research was supported by CERG Grant CityU1004/99P from the Research Grant Council of Hong Kong.

Table 2. Cancer types in the traidobronchial tree calculated for background levels of radiation*.

Cancer type	Frequency appearance (%)	Origin					
		BB (% of total)		Bb (% of total)		AI (% of total)	
Squamous	40	4/5	32	1/5	8	–	–
Small	20	4/5	16	1/5	4	–	–
Adenocarcinoma	35	1/4	8.75	3/4	6.25	–	–
Large	5	1/2	2.5	1/4	1.25	1/4	1.25
Total (%)	100	59.25		39.5		1.25	

* ICRP66 (1994), pp. 33 and 34.

References

- HARLEY, N. H., 1988, Interaction of α -particles with bronchial cells. *Health Physics*, **55**, 665–669.
- HUI, T. E., POSTON, J. W. and FISHER, D. R., 1990, The microdosimetry of radon decay products in the respiratory tract. *Radiation Protection Dosimetry*, **31**, 405–411.
- ICRP, 1994, *Human Respiratory Tract Model for Radiological Protection: A Report of a Task Group of the International Commission on Radiological Protection*. Report 66 (Oxford: Pergamon Press).
- INTERNATIONAL COMMISSION OF RADIATION UNITS AND MEASUREMENTS, 1993, *Stopping Powers and Ranges for Protons and Alpha Particles*. Report 49 (Maryland: ICRU).
- MARSH, J. W. and BIRCHALL, A., 2000, Sensitivity analysis of the weighted equivalent lung dose per unit exposure from radon progeny. *Radiation Protection Dosimetry*, **87**, 167–178.
- MERCER, R. R., RUSSEL, M. L. and CRAPO, J. D., 1991, Radon dosimetry based on the depth distribution of nuclei in human and rat lungs. *Health Physics*, **61**, 117–130.
- NATIONAL RESEARCH COUNCIL, 1991, *Comparative Dosimetry of Radon in Mines and Homes. Panel on Dosimetric Assumption Affecting the Application of Radon Risk Estimates* (Washington, DC: National Academy Press).
- REINEKING, A., KNUTSON, E. A., GEORGE, A. C., SOLOMON, S. B., KESTEN, J., BUTTERWECK, G. and PORSTENDORFER, J., 1994, Size distribution of unattached and aerosol—attached short lived radon decay products: some results of intercomparison measurements. *Radiation Protection Dosimetry*, **56**, 113–118.